2021

Design, Fabrication, and Testing of a High-Speed, Low-Cost Atomic Force Microscope Housing and Distance Measurement System

Jonathan Menke
Minnesota State University, Mankato

Design, Fabrication, and Testing of a High-Speed, Low-Cost Atomic Force Microscope Housing and Distance Measurement System

By

Jonathan Menke

A Senior Thesis Submitted in Partial Fulfillment of the

Requirements for the Degree of

Bachelor of Science

in

Engineering with a Mechatronics Focus

Minnesota State University, Mankato

Mankato, Minnesota

March 2021

March 23rd 2021

Design, Fabrication, and Testing of a High-Speed, Low-Cost Atomic Force Microscope Housing and Distance Measurement System

Jonathan Menke

This Senior Thesis has been examined and approved by the following members of the student's committee.

____

Dr. Robert Sleezer

____

Dr. Rebecca Bates

____

Dr. Jacob Swanson

Abstract

Jonathan Menke: Design, Fabrication, and Testing of a High-Speed, Low-Cost
Atomic Force Microscope Housing and Distance Measurement System
(under the direction of Robert Sleezer)

Advances to the state-of-the-art in fields like biology and material science often stand on the foundation of improved imaging. Here a low-cost Atomic Force Microscope (AFM) housing and distance measurement system was designed, fabricated, and tested. The instrument was developed around an Optical Pickup Unit (OPU) and designed for use as part of a high-speed AFM system. A structure to align the OPU with the probe holder was designed to ensure the beam of the OPU is positioned above the probe in addition to accommodating space, manufacturability, and cost constraints by using cost effective components. The designs were fabricated and assembled before being tested for accuracy and reliability. The results yielded promising characteristics for the prototype demonstrating the capability of measuring 12.5 nanometers with the likelihood of further decreases with the implementation of proper noise isolation.

Acknowledgements

I would like to thank my professors Dr. Sleezer and Dr. Bates who demonstrated infinite patience while guiding me through this thesis from beginning to end. I also thank my parents, Terri and Steve, for supporting me and helping make this thesis possible. Additionally, I also thank the people who helped produce the pieces developed in this theses, Mikkel Schwartz for the PCB development and Keith Alton for the fabrication of the test stand pieces. I would also like to thank my friends and colleagues for their support and assistance throughout this project.

Table of Contents

Chapter 1: Introduction

In today's world our lives are continually improved through advancements and knowledge gained at a smaller and smaller scale. Since the 1600s microscopes have been progressively upgraded to improve our ability to learn about the microscopic universe, the results of which have culminated in the highly sophisticated instruments of the modern era. These instruments allow the world to examine matter at subatomic levels in hopes of enlightening our lives and improving the world. Advancements in STEM fields are often made through the ability to study the world from different angles and under different circumstances. To understand the world's interactions, microscopes have been iterated on to provide increases in resolution and ease of use. Throughout their maturation, strengths and weaknesses to each instrument constructed have driven advancements and improvements that continue to drive research to this day. The main three instrument types that encompass a gross majority of the development in microscopy deal with optical, electron and scanning probe forms of observation. Individually each present their strengths, however their limitations inspire continuous improvement and replacement.

1.1 Advantages and Limitations of Microscopy

Optical microscopes have had limited resolution and are used in identification of features on the order of 200nm due to their reliance on visible light. For many sample types, this instrument is a reasonable outfit, however 200nm is a hard limit [1]. Optical microscopes have been expanded to use X-ray light; however, with the destructive nature of the high energy photons that compose the X-ray band of light, only one image may be ascertained from sensitive samples before they are destroyed. Sample types such as those which are biological are obliterated while taking the first image. Optical microscopes of this caliber are often priced in excess of $30 thousand.

Electron microscopes operate on a similar principle to optical microscopes except that photons are replaced with electrons and magnetic lenses are used. While electron microscopes have 10,000x the resolution of their visible-light optical microscope counterpart, they are limited by their price, portability, and sample types. Electron microscopes are remarkably heavy and immobile and require samples be prepared in a special manner to allow the electron beam to pass through the detector. Furthermore, electron microscopes have an initial capital investment on the order of $50 thousand to $200 thousand [2].

Scanning probe microscopes (SPM) are distinct from other microscopes. These instruments operate in a different way than the others. A scanning probe is based on the observation of how matter interacts with matter. A sample is imaged through observing the movement of a sharp tip as the tip is moved across the surface, either in contact or close to in contact with the sample. Topography of the surface is obtained by the organizing of each line of data that is sampled into a composite image consisting of the data gathered for the entire surface. SPM systems usability are held back by many of the same challenges that face those of optical and electron microscopes, often being heavy and immobile and costing upwards of $100 thousand dollars.

1.2 Objectives

One type of scanning probe microscope is an atomic force microscope (AFM). Its name is derived from the physical contact present between the probe's tip and the surface. The work discussed in this thesis was performed as expansion of previous work performed to develop a low cost, portable and high-speed atomic force microscope capable of resolution comparable with traditional atomic force microscopes. The prior work performed by previous Twin Cities Engineering Program students involved proof of concept work to utilize readily available components that could be used as a stepping stone for the future creation of a low-cost atomic force microscope. The work presented here represents progress toward building an operational prototype AFM using easily sourceable and/or manufacturable components by iterating on previous AFM experimentation work through the use of improved manufacturing methods for electronic components, and through design, manufacturing, and testing of a low-cost AFM component housing.

Chapter 2: Background

2.1 Overview and AFM Instrumentation

The operating principle for scanning probe microscopy is the collection of data about the surface's topography by means of observing the reaction of a probe as it is traced back and forth over the chosen surface until the surface's area is covered. The probe's reaction to traversing the surface is observed and recorded such that the height for each part of the surface is known. A composite topographical image is created through assembly of each data point that was collected.

In atomic force microscopy a finely tipped probe is used to physically contact the surface. As the probe is rastered across the surface, deflection of the cantilever corresponds to changes in surface topography. Two methods of observing cantilever deflection encompass a majority of AFM systems—reflection location observation and reflection shape observation. In the first method the location of the reflection of the beam as it reflects off of the cantilever is correlated to the deflection of the cantilever, and in the second method after the light reflects off the cantilever a light beam's shape is recorded and corresponds to the cantilever's deflection. In both systems the probe in the AFM is rastered across the surface until data for the entire surface is gathered. The data collected allows for topographical images to be constructed of the scanned surface.

2.2 System Overview - Low Cost AFM Approach

The AFM system that this thesis explores uses the reflection shape observation method, where the shape of the reflection correlates to cantilever deflection. To achieve this, circuitry capable of accessing this data and amplifying it appropriately accompanies an Optical Pickup Unit (OPU). A completed system leverages the precision of the OPU's ability to detect small changes in elevation of the probe. The OPU produces a beam of infrared light which is to be reflected off the back of the cantilever of the probe. The shape of the beam is detected with a photodiode array. The specifics about the OPU function are discussed in the OPU section of the Background section. A flow diagram for data processing and acquisition is shown in Figure 1.

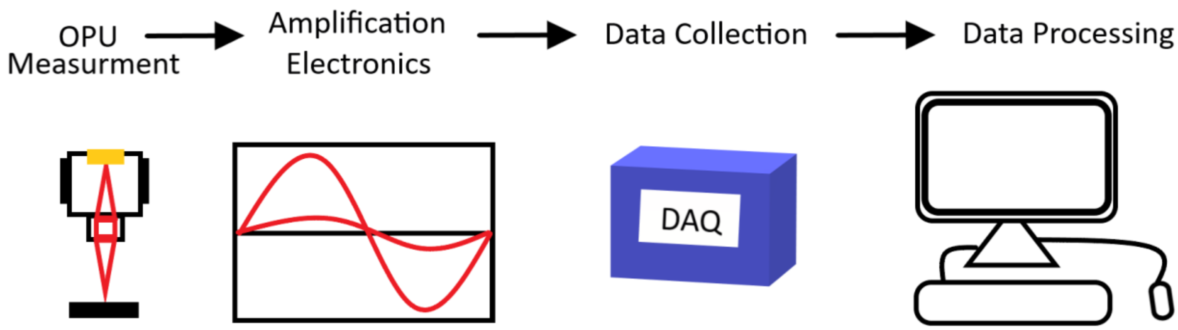

Figure 1: Flow diagram for data amplification, acquisition, and processing

2.2.1 Component 1: Probe

The probe in an atomic force microscope is generated through a multistep silicon etching process where the final product is designed specifically for use with atomic force microscopes [3]. The three primary components of the probe are the tip, the cantilever, and the holder. The tip portion is the part of the probe that comes into contact with the sample and its exceptionally small form factor allows it to contact only a small area of a sample at a time. The vertical movement of the tip during sampling is transferred to the cantilever. The cantilever, being much larger than the tip, is the primary instrument used for acquisition of an image. Light from the light source reflects off the back of the cantilever and into a receiver. The holder for the probe has its purpose as the method of attachment to the remainder of the AFM system. Figure 2 provides an example of a probe as well as some general values for typical configurations.

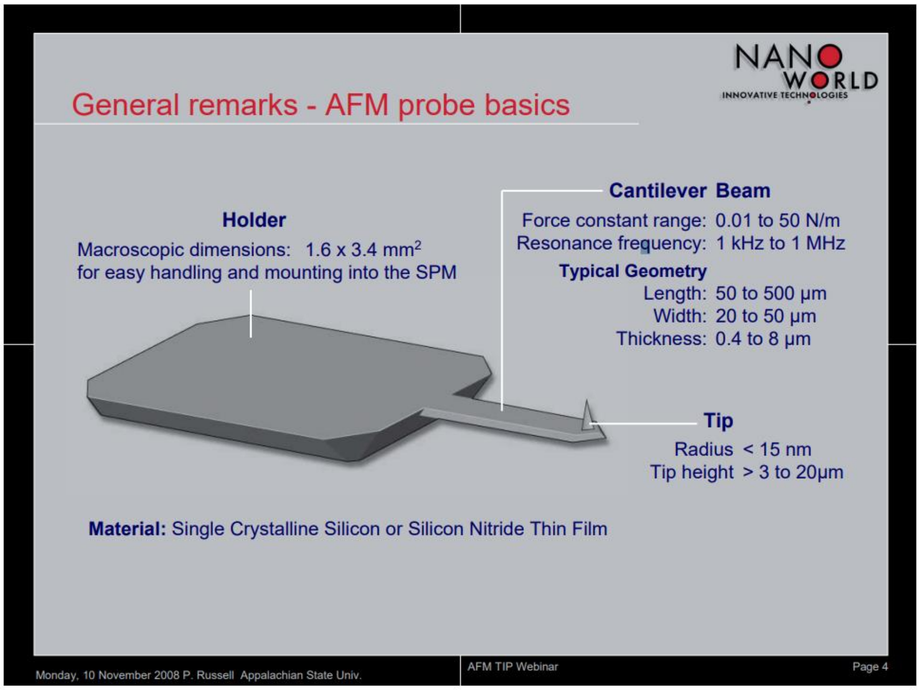

Figure 2: Atomic Force Microscope Probe Basics [3]

2.2.2 Component 2: Emitter and Photodiode (OPU)

An Emitter in an OPU produces a beam of infrared light with a wavelength of 760nm to 800nm [4] which leaves the OPU and is focused on the back of the cantilever. The beam then reflects back into the OPU where its shape is captured with a photodiode array composed of four quadrants. The intensity of light detected in each quadrant corresponds to the cantilever's position relative to the focal point of the OPU which can be visualized in Figure 2. Due to the configuration of the lenses an astigmatic beam is produced such that the distance to the surface is determined based on the shape of that beam on a specific plane.

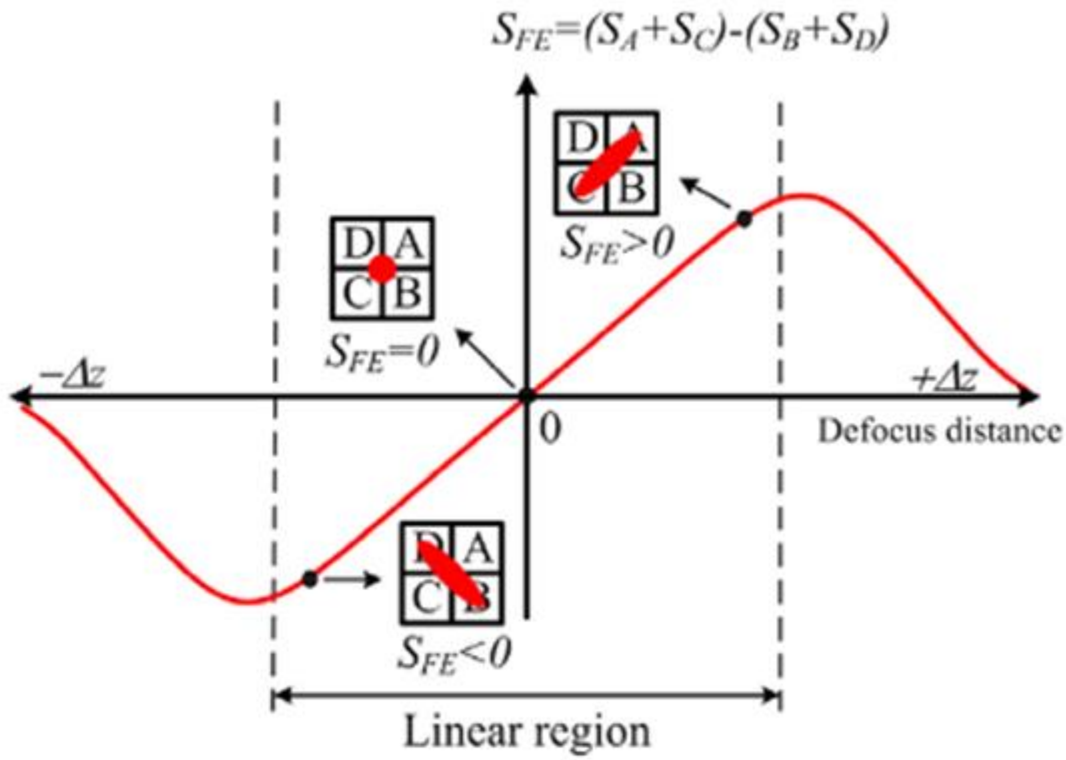

Figure 3: Photodiode light collection in contrast to the cantilever's distance relative to the OPU focal point [5].

The cantilever's movement through the focal point is shown in the diagram above in Figure 3 where the relative location of the cantilever is extrapolated using the Formula:

$$\text{Height} \propto (A + C) - (B + D) \tag{1}$$

Which is rearranged as:

$$\text{Height} \propto (A - B) + (C - D) \tag{2}$$

The transformation of Equation 1 into Equation 2 allows for the equations easier integration into a circuit. Using two differential voltage amplifiers and a summation amplifier allows the equation to be executed physically in hardware while simultaneously allowing for the amplification of the signals such that they are able to be easily collected and processed [6].

2.2.3 Component 3: Sample

In atomic force microscopes, samples are limited by their ability to be in contact with the probe. Rigid samples such as metals and silicon often work well with little to no preparation, though soft samples such as organisms or particular matter are also able to be measured. These non-rigid samples require simple preparation with a substrate such as mica, a clean and flat work space, and constraining of the movement of the sample. One of the greatest strengths for collecting data using AFM methods is the ability to measure samples without interfering with the sample's natural state. Living samples are capable of being measured due to the minimally intrusive techniques for sample preparation and observation [7]. In comparison with other high resolution microscopy techniques such as electron or X-ray, the sample is not destroyed, which allows for more than a snapshot of the sample to be imaged and for changes to be observed over time [8].

2.2.4 Component 4: Sample Holder/Positioner

Atomic force microscopes require precise alignment mechanisms to position the tip of the probe gently on the surface of the sample. To move the sample to the probe, compounding positioners are necessary to achieve precision. First a micrometer is used to move the sample in the Z direction to a location in close proximity to the probe tip, and then a piezo actuator will bring the sample into contact with the probe. To image the surface once positioned, a set of piezo actuators operate in the X and Y directions to raster the sample relative to the probe tip so that the desired section of the surface area is entirely scanned.

2.3 System Integration

The components in the AFM system must be aligned for the system to function. Balancing each component's operating range is preferred so that each component is close to a neutral position when the instrument is powered on and no component is at one of its extremes. If any one component is at its extremes during initial setup it may prevent the ability to tune the system, interfering with operation. The neutral point of the optical element of the AFM needs to have the beam aligned onto the cantilever and have it reflect on to the laser's receptacle in a balanced manner. Essentially the focal point of the OPU laser should be placed on the cantilever when the cantilever's tip is in contact with the sample surface and the cantilever is deflecting due to the tips contact, while still in a relatively neutral position. Development of a system where each component exists comfortably close to its neutral position, such that tuning may occur upon use, is a primary driving factor for developing a properly integrable and functional AFM system.

2.3.1 Probe Movement - Alignment

The alignment of the probe under the cantilever is a process that involves aligning the thin beam emitted from the laser diode onto the cantilever. To achieve alignment screw based linear actuators are used. The linear actuators move the cantilever and/or OPU until the photodiode array detects its presence. Changes in light detected in the photodiode are indications of the probe having passed near the focal point of the OPU. Further tuning using trial and error is used to position the beam near the edge of the cantilever near the probe tip, such as seen in Figure 4.

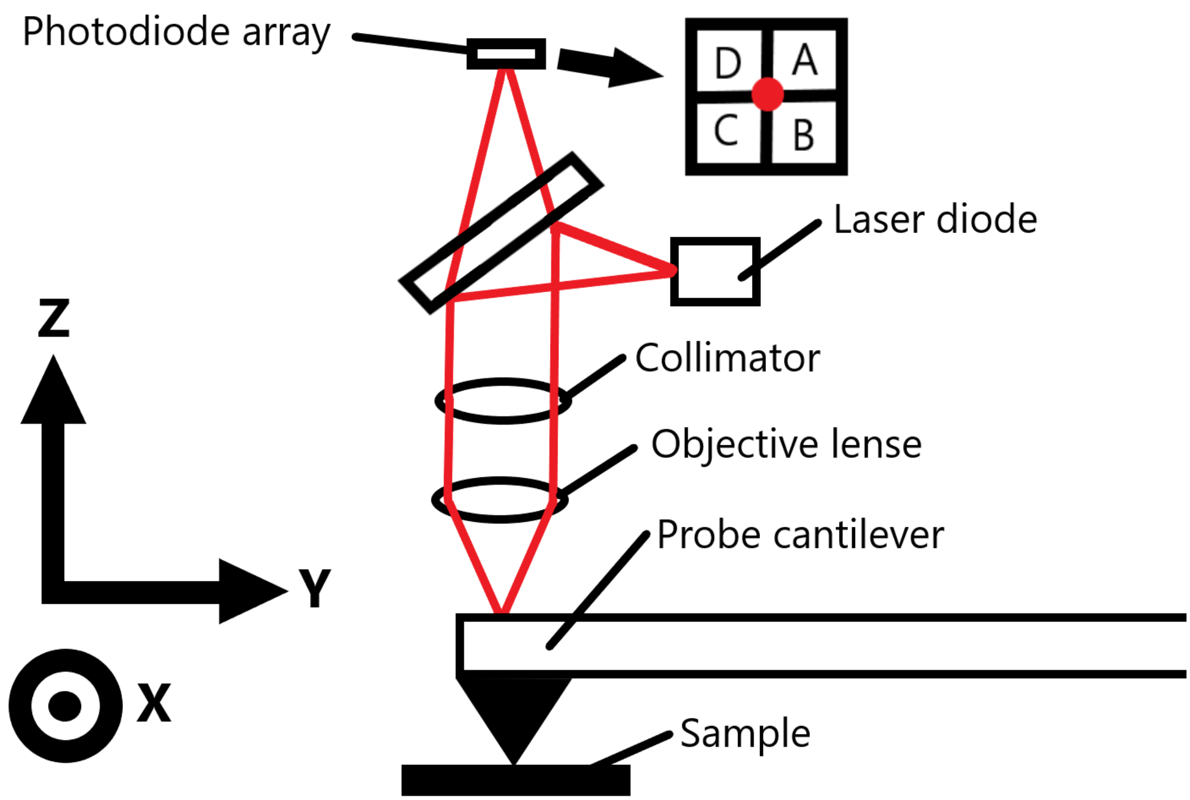

Figure 4: Beam reflection shape observation based atomic force microscope configuration (not to scale)

2.3.2 Tuning/Alignment Characteristics

Tuning the system involves the process of aligning the system components gradually and more finely until the movement of the cantilever is detected by the OPU and then gradually moved into a position. AFM systems use adjustment mechanisms on each component to allow this to occur. The probe holder, the OPU and the sample each have adjusters with high enough accuracy to allow for consistent miniscule alignments. Tuning requires a trial-and-error method, moving the beam until its reflection is detected in the neutral position on the cantilever and while the cantilever is also in a relatively neutral position. Meaning that the cantilever is touching the sample but is not over strained by its contact.

2.4 Low-Cost Atomic Force Microscopes

Building low-cost AFMs is not a new development. Other groups have progressed and developed the premise behind developing low-cost and small AFMs; however, while it has been done, and there are examples of products that have been brought to market, these instruments have reduced resolution. The resolution is orders of magnitude lower than the theoretical resolution limits found in their precision-based expensive counterparts. While these instruments are exceptional in many ways, they lack the precision needed to assist in finding new discoveries at the atomic level. One such instrument developed by the students in Shenzhen finds itself cheaper than the expensive alternatives and is relatively easy to assemble and manufacture. While it is simple to operate, it is unable to discern details smaller than 1 micrometer. The Shenzhen group followed the approach of using an OPU, and a combination of an Arduino and an interceptor board to control the AFM. Ultimately, their system configuration heavily limited the resolution in an attempt to allow for a more robust instrument that can be more easily and cheaply fabricated [9].

Other attempts at AFMs have produced promising results with exceptional resolution on the order of 10 nanometers. ICSPI's nGauge AFM demonstrated that form factor and cost are not limitations to the ability to acquire data on the nanoscale, proving that despite its small form factor, high quality data can still be obtained [10]. One of the primary drawbacks of this system is imaging speed. Where several images per second would be desirable, due to their component configuration and design choices, this is unattainable.

Further attempts at low cost AFMs involve the use of a quantum tuning fork in place of a beam and receptacle method. While allowing for more compact operation, implementing a low-cost AFM with a tuning fork limits resolution [11]. Furthermore, the quartz tuning forks appropriate for this application are challenging to obtain. The main principle behind a quantum tuning fork-based AFM operation is modulation of a vertical piezo actuator while the probe tip is close to the sample surface. The AFM uses a PID controller to maintain a consistent distance to the surface in response to changes in the quantum tuning fork's resonance amplitude which changes when the probe tip is closer or farther from the surface. While in the sampling process, the surface topography is correlated to the changes in the piezo actuator's height. Because the piezo height is controlled by the PID controller, a composite image of the surface can be created based on the PID controller's responses and the quantum tuning fork's resonance amplitude change data.

Often the designers of low cost AFMs focus on producibility and ease of marketing rather than functionality. Many low-cost AFMs available to the public have reduced resolution and scanning speed as a tradeoff for robustness and scale of production.

2.4.1 Improving Accuracy

Achieving relatively high degrees of accuracy in AFMs is often a principal concern. While AFMs provide distinct benefits, other imaging methods also have considerable benefits, while also having had time to mature. Throughout AFM development history, several innovative methods were developed to further increase the accuracy of these systems. This includes altering several facets of the AFM process through manipulation of the control systems, introduction of new parts and variables, as well as alteration of components [12], [13], [14]. Additionally, environmental changes and noise considerations have been explored as solutions for further increases in resolution.

One of the preferred methods of improvement in accuracy is through improvement in the noise floor by isolating the device from interference from outside forces such as air vibrations and electrical interference [15]. This can be done by using physical barriers such as noise isolation chambers and/or moving away from loud and crowded environments, even going so far as to construct dedicated buildings. This isolation assists in creating a low energy environment, helping to lower the noise floor and increase resolution and accuracy.

Further noise reduction can be achieved with changes to the control and sensor circuitry to correct for the non-ideal performance in components. Special circuitry configurations such as those discussed in EMI prevention documentation can also be utilized to further isolate the circuit noise [16].

Some groups have implemented multicomponent feedback sensors with PID controlled nano positioners to account for the drifts involved in alignment of components [17]. Ultimately, these controllers rapidly compensate for creep, hysteresis, and thermal noise at the nanoscale to maintain alignment throughout use of the AFM. The PID controllers compensate for the noise introduced by the changing and predicable behavior of the components, keeping the system aligned, and generating a higher degree of reliability and accuracy.

Downforce on the cantilever of the probe as a means of keeping the tip in contact with the surface while scanning has been found as one method of increasing accuracy. This technique operates on the principle that reducing the amount of time it takes the cantilever to return to the surface during use creates a more complete image with higher resolution features. Applying force to the cantilever was demonstrated to increase accuracy in tests by about 20%. By keeping the probe in contact using downforce, the probe remains in position on the surface due to the increased energy required to lift the probe. This means that noise would have to rise to a greater level before its presence would be felt in the data [15], [18].

2.4.2 Improving Reliability

Reliability improvements stem from addressing problems as they arise. Engineers perform routine tests and fix problems as they occur and develop solutions to prevent failure in the future. While some may argue that reliability and accuracy are mutually exclusive achievements, the goal is to maximize both. If components wear down, their consistency becomes questionable. A key factor for reliability is acquiring components designed for prolonged use, as well as regular replacement of components that fall out of alignment over time.

Transportation of systems is often an overlooked challenge and introduces variance in the components. During transport the systems are stressed in unpredictable ways, and precautions must be taken to ensure each component is capable of managing the challenges of transport. The systems must be continually robust through the duration of transport.

The mechanical components of an AFM are important factors to the reliability of the system, but without the electrical equipment to support the AFM, the AFM won't function. Ensuring that protections and precautions are in place to prevent failure of any developed electrical equipment is a vital step toward reliability improvements. Examples of failure protections have been through the implementation of Electro Static Discharge (ESD) mitigation techniques to prevent damage to the system through changes to the circuit's design [19], [20]. The AFM circuitry systems are particularly sensitive to noise. In addition to the circuitry having to be properly maintained, each of the circuit components' temperature characteristics must be accounted for. Temperature affects the integrity of the data signals, impacting the reliability of the results [21].

2.4.3 Noise Literature Review

Reducing the presence of a noise floor is vital to reaching new levels of accuracy. Many components that help the instrument function also impede its ability to perform through the introduction of noise. Noise in this instance is the presence of non-valuable information being intertwined with the information that needs to be captured. Noise exists as a collection of the chaos that can be sometimes controlled. Electrical, vibration and thermal interferences are the primary offenders in causing noise, and while it would be beneficial to understand all the factors that impact the system, the focus here will be on the factors that are most controllable given the low-cost development environment.

Electrical noise stems from approximations made when designing a circuit [22]. The treatment of real components as their ideal counterparts leads to EMI susceptibility. Due to the innate electrical-magnetic behavior of all transmission lines, every wire becomes an antenna and an emitter, and for this reason breadboards are thrown out as a plausible idea if precise work is to be achieved.

Furthermore, when designing circuit boards several factors must be accounted for so that unwanted behaviors such as parasitics and cross-talk are minimized [23]. Additionally, the presence of capacitors in strategic locations can be used to greatly reduce and filter spikes and noise, improve power delivery to components, and maintain reasonable signal integrity.

Vibrational noise is also very common, and physical isolation from the outside world is one of the principal solutions; however, in many cases physical isolation is not viable. The introduction of physical vibrations, even small ones, have significant impacts on the ability to measure on the nanoscale [23]. Even the presence of people across the room in the background has enough impact to be more than noticeable by these sensitive instruments. A principal solution then becomes to work in a quiet environment and take precautions to isolate the instrument from incoming noise, by placing the instrument on a heavy object and isolating the AFM in a room by itself.

The stimulation of the air surrounding the AFM can introduce noise which will manifest itself in the data even when the unit is physically isolated [25]. Disruption due to loud noises also impacts the ability for these systems to function and provide clear data. Acoustic noise may couple to surfaces and resonate portions of the instrument, ultimately intruding data in the signal. To reduce noise the system should be placed in a low energy environment free from typical extraneous energy and noise.

The low-cost OPUs also present their own challenges since they are manufactured for use in a different environment. Because they are not specifically designed for use with AFMs some parts of the OPUs have inconsistent ability to tolerate noise and have inconsistent response characteristics which impact the accuracy of measurements. Additionally, the photodiode sensor in the OPU is designed to respond to a set bandwidth of light. The introduction of additional light sources that operate in that same bandwidth have the capacity to influence the results through the introduction of additional noise [4]. Furthermore, fluctuations in power delivery can influence the behavior of the emitter diode, which would cause further light based noise in the AFM. Achieving a steady power delivery and reducing fluctuations in light levels from all sources should greatly reduce the likelihood of trouble stemming from the photodiode’s sensitivity to light level fluctuation.

2.4.4 Previous Research Conducted by Twin Cities Engineering Students

The work completed by other Twin Cities Engineering students has been used as a foundation for pursuing further development of OPU based AFM research [6], [26]. The initial work involved the testing of an off-the-shelf OPU as a means of measuring changes in movement of a surface through the focal point of the OPU. Ultimately their work provided a basis for understanding the signals generated by the OPU, which student researchers concluded was an acceptable device for use in a low-cost AFMs. Their testing revealed the sensitivity and applicability of the OPU in future development.

Furthermore, Justin Rudie, an undergraduate student in the Twin Cities Engineering program made additional progress by developing a more advanced prototype that is pictured in

Figure 5. The progress that he made was the basis for the efforts presented in this thesis. Rudie's efforts were directed toward measurement and amplification of the output signals generated by the OPU [6]. This system used an amplification circuit that generated an output waveform based on the signals generated by the photodiode array in the OPU. Due to the form factor of the photodiode array in the OPU, the quantity of light being detected in each quadrant corresponds with the distance the surface is from the focal point. As the light is shined and is reflected down onto a surface, the distance to the surface determines the shape of the light when it is detected by the photodiode array. Quadrants, marked A, B, C, and D, are arranged in a square. The output voltage in each quadrant corresponds to the intensity of light absorbed and thus the distance is extrapolated based on the status of these four voltages.

Rudie worked to amplify the signals captured by the photodiode array and built a circuit capable of differentiating between the small differences in signal voltages and then combining them appropriately and amplifying their output so they could be captured with a Data Acquisition (DAQ) device. The circuit implemented Equation 2, as discussed previously, while also amplifying the difference in the photodiode quadrant signal approximately 4,130 times.

This circuit's output corresponds to the change in distance to the surface as detected by the photodiode array. Under the ideal conditions Rudie's system was able to discern 12.5nm of resolution.

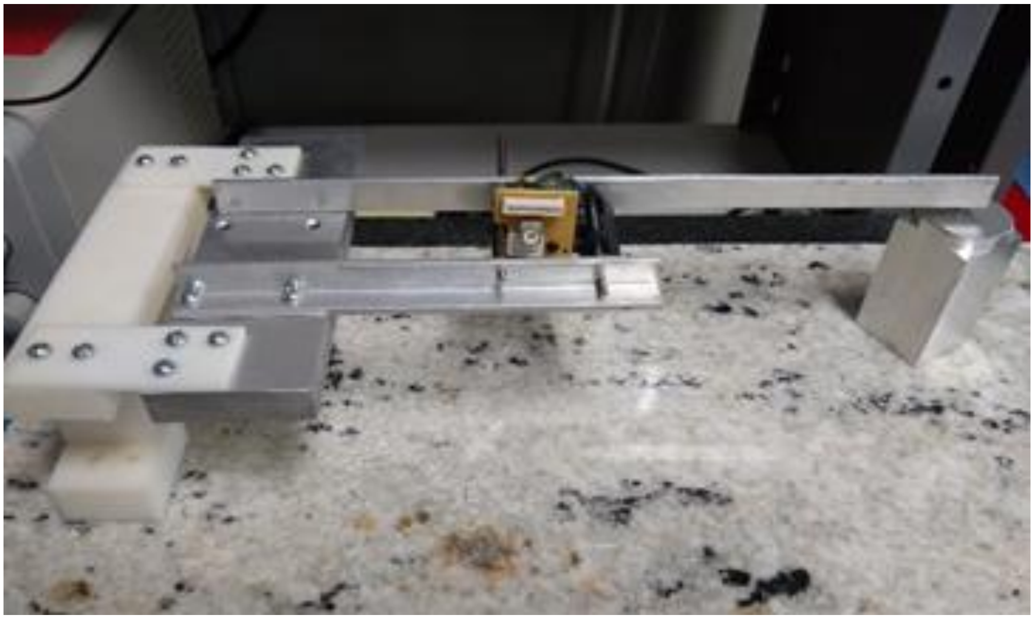
Figure 5: Justin Rudie’s Optical Pickup Unit and Test Stand [6]

Due to the prototype nature of Rudie’s circuit configuration, consistent results were intermittent. Because it was implemented on a breadboard, its output characteristics were inconsistent and the reliability had room for improvement. Additionally, the unit was constructed with several wires acting as antennas which were believed to contribute to the elevation of the noise floor. Furthermore, the power delivery system was thermally inconsistent, leading to initial fluctuations in power delivery to the OPU, and inconsistency in amplification.

Neither the stand nor the circuit were designed to be used with an AFM probe. While the results did demonstrate a proof of concept, the device demonstrated a need for it to be redesigned for implementation as an AFM.

Despite its deficiencies, as a whole, the stand and the circuit worked as intended and confirmed the ability to properly acquire and amplify signals produced by the OPU. Ultimately the next steps towards building a functional AFM was iterating on this device and improving each component with a primary focus on aligning each component in the AFM and properly amplifying the data so that it may be recorded.

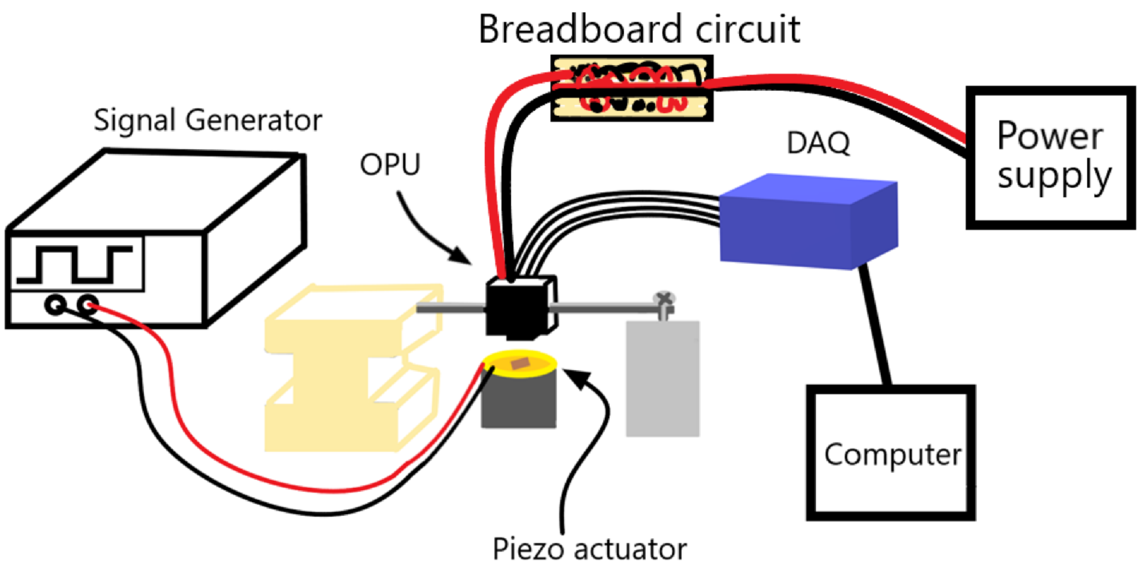

Figure 6: Testing setup using Rudie's prototype

Approaching Rudie's system, efforts were made to better quantify the challenges inherent to Rudie's prototype test stand and circuit. Measurements were made to quantify the noise and thermal drift, to be used as a reference in the future. These experiments using Rudie's system involved oscillating the piezo in a square wave and recording the data with a DAQ device. The square wave with a 1V amplitude was used to visualize vertical focal drift should it occur. Under perfect circumstances the graph's line, which is generated using the collected data, would be completely horizontal and of uniform zero width due to the values received in each quadrant canceling their respective peaks and troughs caused by the oscillating piezo. The setup is shown in Figure 6.

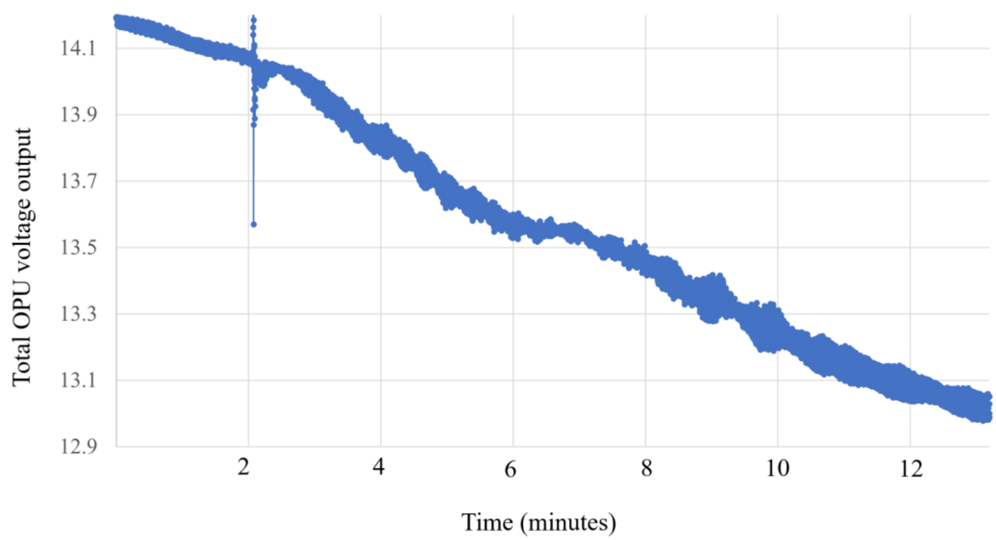

Figure 7: Graph: Summed OPU voltage outputs over time.
Vertical Axis: volts, Horizontal axis: minutes.

The data in Figure 7 corresponds to the voltage over time being outputted by the OPU as received by the DAQ. In this test the voltage outputs from each quadrant are added together in software after their collection to obtain a general performance metric for consistency of the circuit.

Using the graph above as a baseline for general behavior for Rudie's system, two major trends present themselves — a systematic general downward trend in the total voltage output, and the intermittent oscillations in voltage along the downward trend indicating issues with maintaining vertical focal distance. One challenge that Rudie battled was consistency with power delivery. These results seem to validate that concern. Additionally, the fluctuation in the thickness of the line is cause for concern for the overall susceptibility to noise and disturbances and would seem to indicate that implementing general improvements to reduce EMI and noise susceptibility as a whole would benefit the instrument. Furthermore, changes to the power delivery system would provide an improved relationship between the amplification circuit and the OPU. Consistency across the board should help with reliability.

To achieve a more appropriate AFM configuration the intention was to leverage this knowledge and move forward with the construction of a circuit board for the amplification of the OPU outputs and powering of the OPU, incorporating measures to reduce EMI and noise throughout the system and improving the reliability of the system as a whole. Furthermore, to accompany the circuit, a dedicated test stand for improved noise reduction and for use as an AFM prototype was to be fabricated to accommodate mounting of an OPU and probe alignment mechanism.

Chapter 3: Methodology

The methodology here represents the processes taken to design, implement, and test an improved prototype OPU holder and amplification circuit. This section is divided into design and test methodology. The design methods section discusses the basis for the development of the design prototype test stand and circuit, and the testing methodology section discusses the testing areas for evaluating the design results and compares the design with the prior prototype.

3.1 Design Methodology

To advance this project to the next level, it's important that a goal be established as a marker for what constitutes an iteration of the design. So far this thesis has discussed what others have done, their successes, and the implications on the ability to achieve what was set out as the end goal this thesis. The efforts made in this thesis exist as a stepping stone for future work, and the design methodology used is with that in mind. From what was learned from others, the goal was to build a new prototype instrument where each piece was improved. To achieve this, the circuit controlling the OPU was revised and improved to reduce the concerns for inconsistency present with Rudie's circuit. Moreover, the development of a physical mounting system for use as an AFM was designed in addition to developing the components for aligning the probe under the OPU.

3.1. 1 Circuitry

The primary areas for improving the circuit was with respect to noise reduction, reliability and testability. To achieve this, the development of a Printed Circuit Board (PCB) counterpart to the original breadboard circuit was produced. In doing so, it was expected that a noticeable behavior change would be observable throughout testing. To test the new board, additional probe points at key locations were inserted to allow for easy investigation into the functionality and for troubleshooting.

To ensure that what was built was functional, testing the amplification using simulated OPU outputs was performed. Additionally, the precise amplification could be determined since the circuit board would be more stable compared to the breadboard. Upon completion the expected amplification and actual amplification was expected to slightly differ due to imperfect components, but would likely remain close to what was expected. Obtaining a baseline amplification was performed to aid in quantifying the circuit's functionality. Final testing to confirm functionally included capturing the noise floor of the circuit and examining the nature of the system using a Fast Fourier Transform (FFT) of the circuit's output while intentional stimulation was absent.

The circuit board’s configuration was designed so that most components with the exception of the test point pins would be Surface Mount Devices (SMD). In doing so, additional EMI noise and interference reductions were expected in addition to allowing for the ground work to be laid for future configurations of the circuit board. Knowing signal integrity was important, choosing a SMD based circuit allowed for a smaller and more compact unit that was expected to be less susceptible to EMI.

To achieve this the previous circuit was recreated using ALTIUM software and modified to add capacitors to each of the INA217 amplifiers as specified by the amplifier’s manufacturer. The resulting circuit diagram is seen in Figure 8.

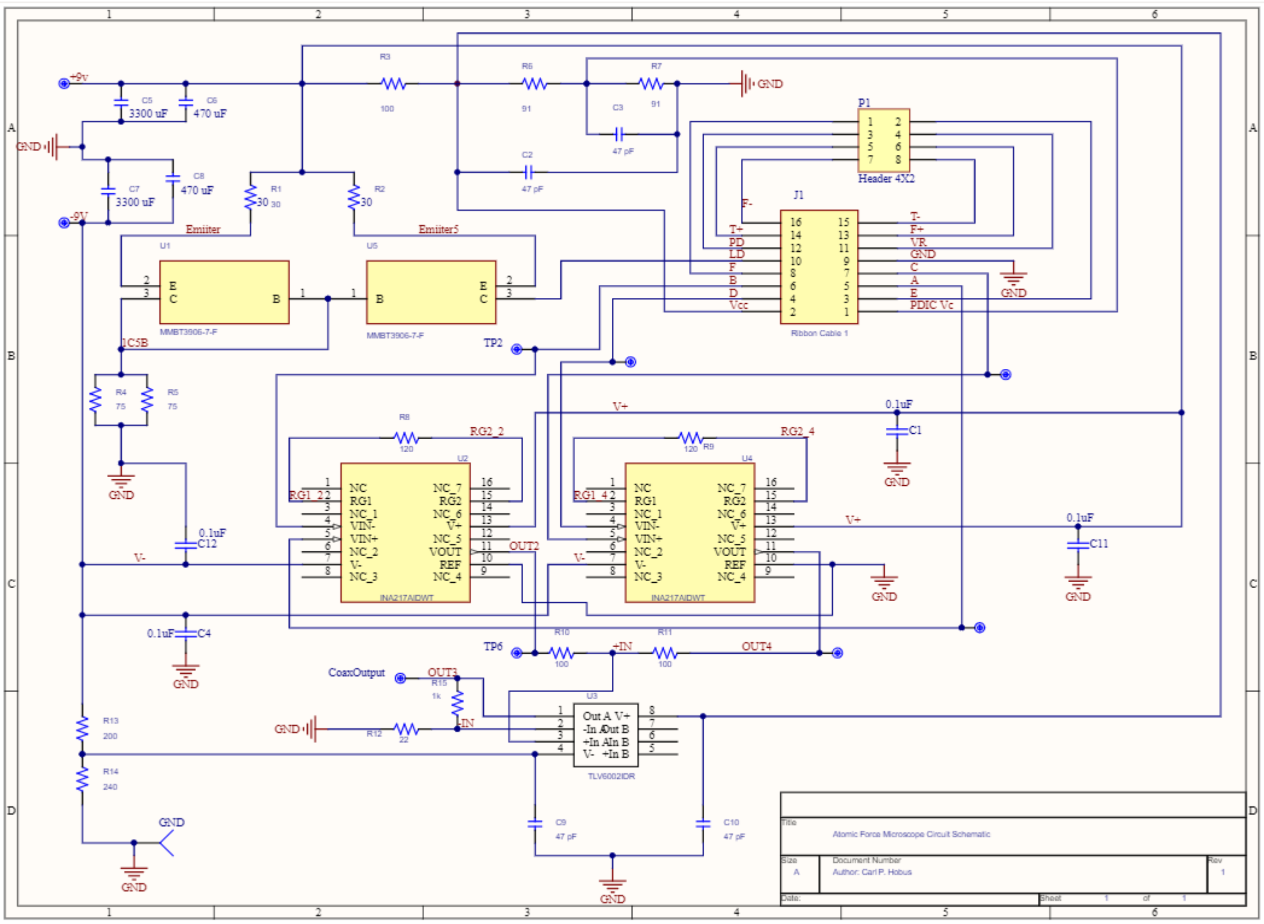

Figure 8: Circuit diagram

In transferring this circuit to a physical layout of the board, basic EMI was taken into consideration and, in an attempt to reduce noise, the lengths of traces were reduced to minimize their effects as antennas. Accounting for the previously discussed design considerations resulted in the circuit layout found in Figure 9, which was printed by Advanced Circuits in Maple Grove, Minnesota.

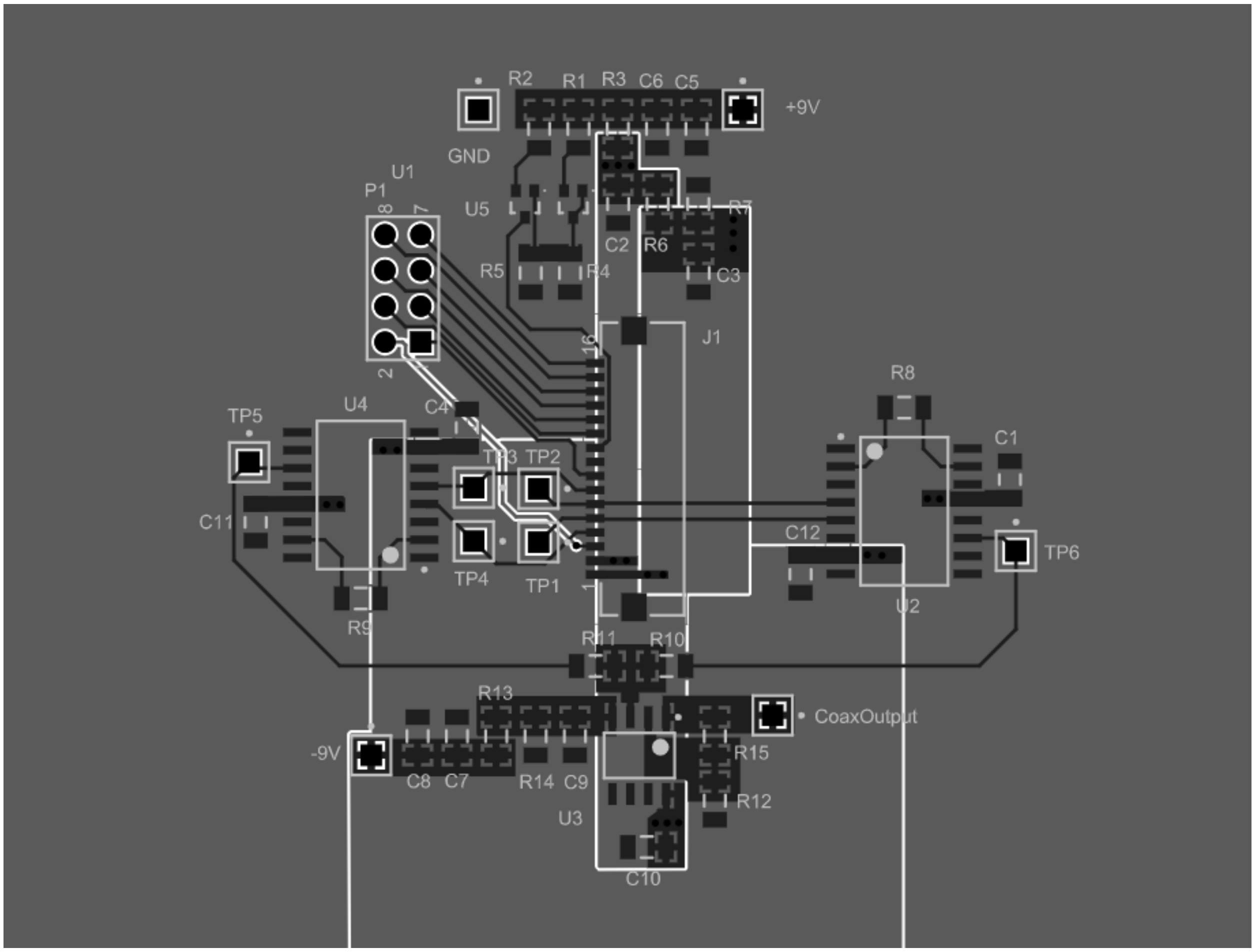

Figure 9: New circuit layout

This two-sided circuit board compacts the circuit and heavily reduces the footprint. Due to the soldered components it was expected that performance would be consistent in addition to being less susceptible to noise and interference that was present in the breadboard implementation. The specific inputs and outputs of this circuit are illustrated below in Table 1 to better convey the nature of the circuit.

Table 1. The list of inputs and outputs of the PCB seen in Figure 9

Connection	***Signal Type***	***Signal Description***
+9V	Power Rail (Input)	DC voltage of 9V ± 0.05V
Ground	Ground (Output)	Ground
-9V	Power Rail (Input)	DC voltage -9V ±0.05V

Table 1 (continued)

A (TP1)	Input and Output	Signal from first quadrant of the photodetector
B (TP2)	Input and Output	Signal from second quadrant of the photodetector
C (TP3)	Input and Output	Signal from third quadrant of the photodetector
D (TP4)	Input and Output	Signal from fourth quadrant of photodetector
E (P1-2)	Input and Output	Signal from photodetector used for focusing and tracking error correction
F (P1-1)	Input and Output	Signal from photodetector used for focusing and tracking error correction
F+ (P1-6)	Input	Positive signal input for changing astigmatic lenses focal point (Focusing)
F- (P1-7)	Input	Negative signal input for changing astigmatic lenses focal point (Focusing)
T+ (P1-5)	Input	Positive signal input for changing horizontal position of the astigmatic lens (Tracking)
T- (P1-8)	Input	Negative signal input for changing horizontal position of the astigmatic lens (Tracking)
Amplified A-B (TP6)	Output	Signal for the amplified difference between Signals A and B
Amplified C-D (TP5)	Output	Signal for the amplified difference between Signals C and D
CoaxOutput (Amplified (A-B)+(C-D))	Output	Signal for the amplified differences between A,B,C, and D, pertaining to position of surface relative to photodetector

3.1.2 Test Stand

In development of the test stand and its supporting components, the freedom with which things could be designed was constrained because the linear actuating stages to be used in this project were already purchased. While a design for a test stand had been developed, it was ultimately incomplete. The prototype needed to be configured to function as an AFM and therefore each component needed to be mounted so that the OPU and probe could be positioned independently, in addition to being capable of being serviced once integrated. To allow this to occur, three other pieces, in addition to the test stand, were designed and fabricated.

Since noise is an important factor and should be minimized, aluminum was chosen as the material of choice for the components in the system due to its relatively balanced rigidity and formability, heft, and cost compared to other accessible materials such as wood, ABS plastic and steel. This aluminum was CNC machined due to its ability to be done so quickly and cost effectively. Furthermore, the aluminum’s mass would help to provide decent noise isolation inherent to the system, and would allow for rigid attachments of components during assembly.

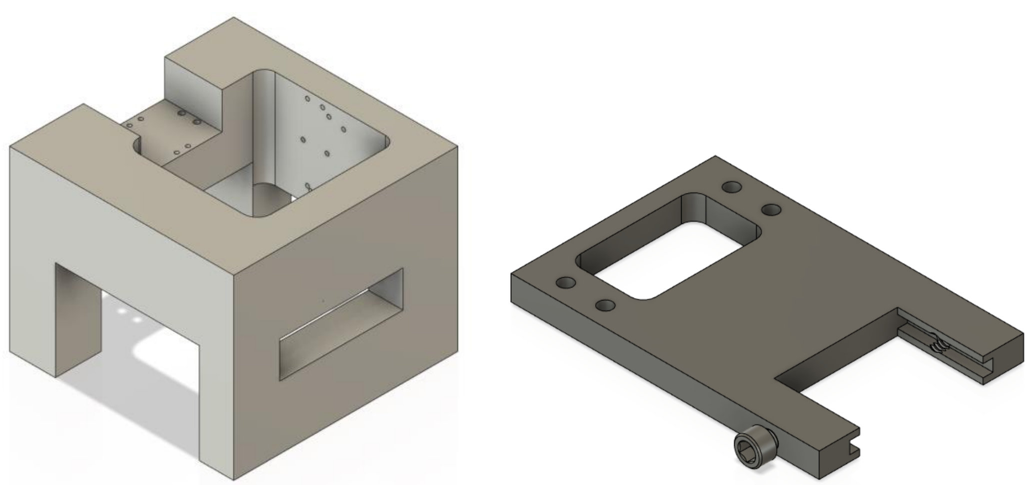

Figure 10: The four machined components from left to right, top to bottom: the test stand, probe holder adapter, linear stage linker, OPU holder.

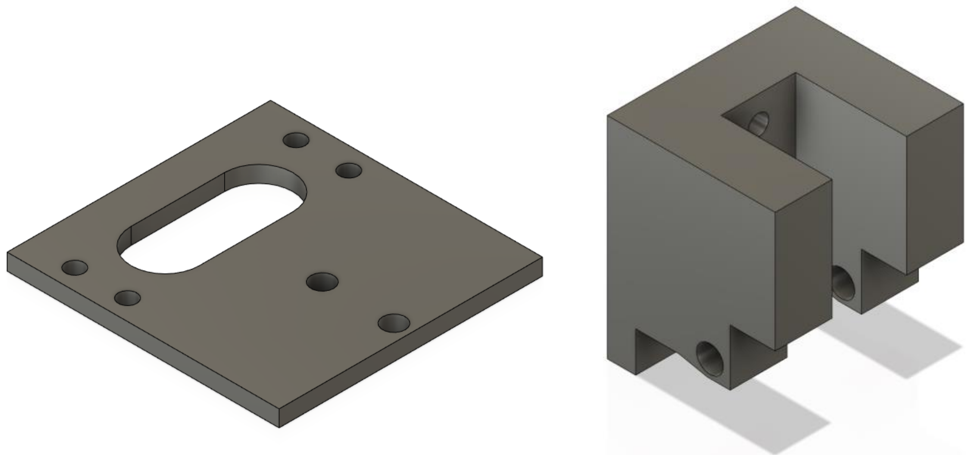

Figure 10: (continued)

The four components seen in Figure 10 were chosen as a means to build the AFM and achieve alignment of the cantilever and the OPU. The first component, the stand itself, is a large rectangular aluminum block with its center removed, its structure chosen due to its stability and heft, reducing movement when contacted, bumped, or moved. The stand's heavy structure is used as a means to reduce its noise footprint. The purpose is to allow for the OPU to be mounted and have it aligned with the probe. For this to occur, the second component was needed. An OPU mounting device was designed to allow the OPU to be attached to a linear stage so that the OPU could be focused and perpendicular to the cantilever.

The final three components designed were for positioning of the probe under the beam of the OPU seen initially in Figure 10 and assembled with the linear stages in Figure 11. Two components in conjunction with two linear stages allow for the probe to be moved in the XY direction, resulting in the ability to focus the probe with the OPU. The component at the bottom, the probe holder adapter, is made to allow for the probe holder to be slid in the front and tightened down with thumb screws to ensure minimal movement. The component is then attached to two linear stages separated by a plate to mount them at 90 degrees of difference. This configuration allows the probe to fully traverse areas where the focal point of the OPU is likely to be.

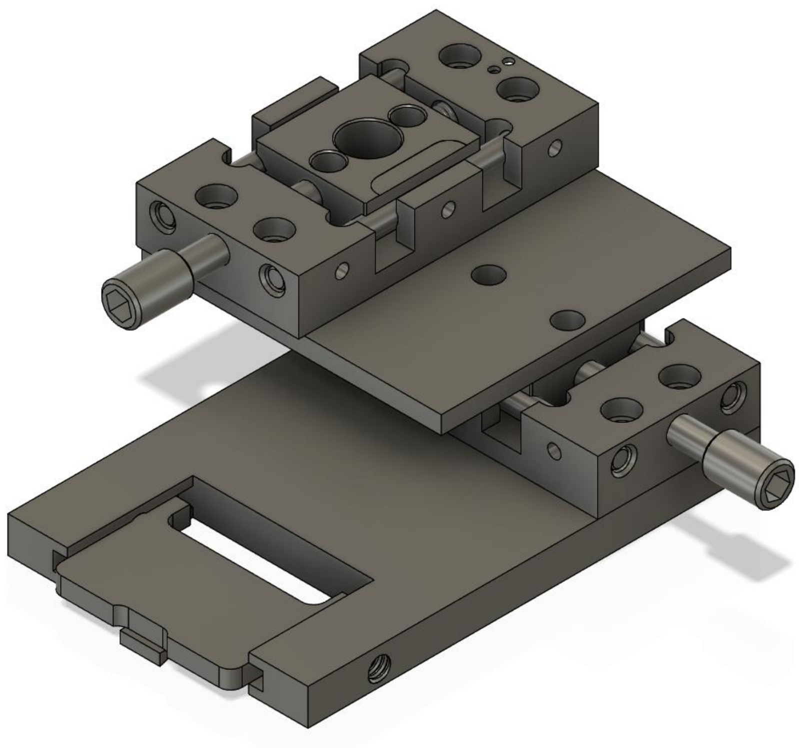

Figure 11: Linear stage linker and probe holder assembled with linear stages

These linear stages were chosen due to the precision needed for alignment of the probe and its holder under the beam of the OPU. While it wasn't expected that the alignment would be easy, it was expected that alignment would be possible given the time and effort. Adjusting these stages in small increments using hex keys placed in each of the turnable knobs and correcting based on the observed effects was the method chosen for achieving alignment. In future iterations, changes to this configuration would likely improve usability, however functionality was the primary concern during this endeavor. A visualization of the assembled configuration is below in Figures 12 and 13.

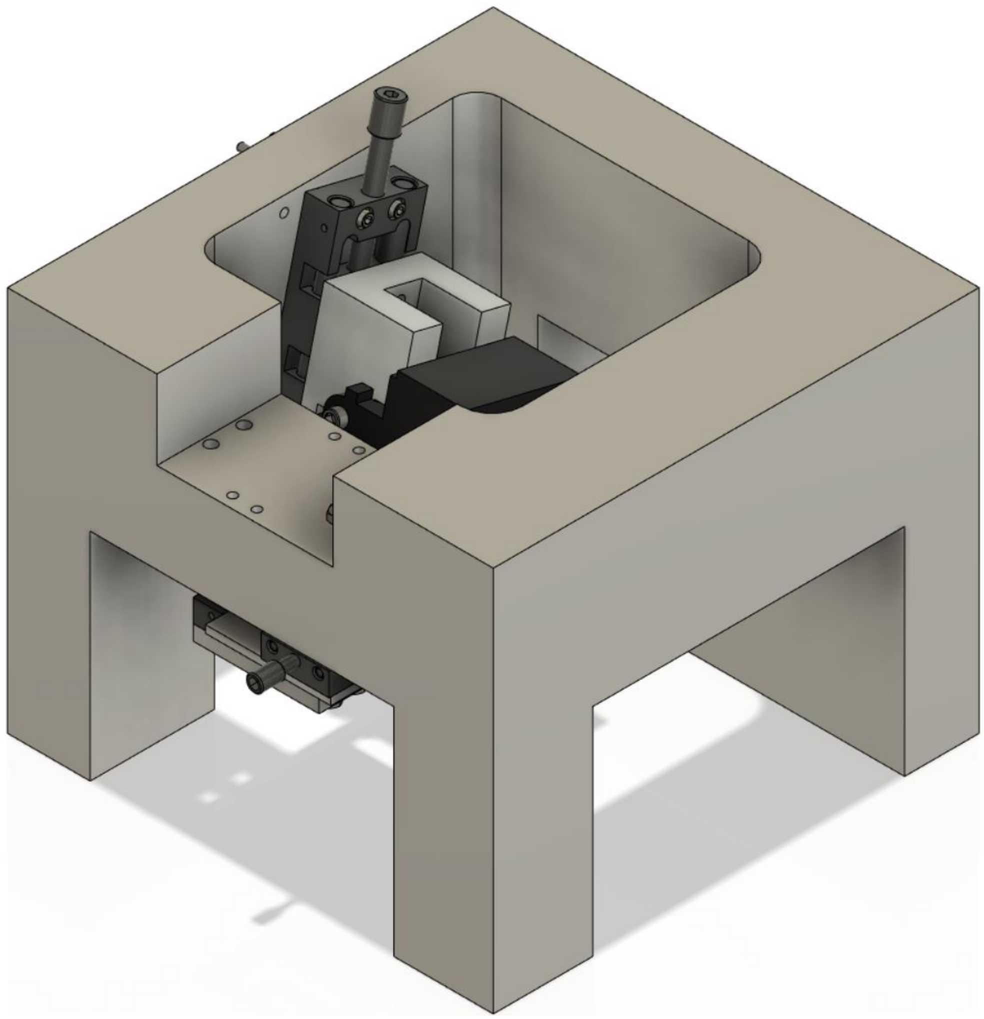

Figure 12: Test stand fully assembled in AFM configuration

One major constraint in the project was with concern for the space availability. The components needed to be in close proximity to each other to allow for alignment which meant that it was essential that components didn't take up unnecessary space. It was important that each component not collide in unforeseen ways during assembly and tuning or they might break. Underneath the probe, the sample and the equipment used to move the sample needed room to be finely positioned whenever used. This meant that the probe positioner should be out of the way of any equipment and the sample as it is moved into position and brought up to the probe. This assembly configuration achieved acceptable clearance and the allotted clearance for the sample and equipment is seen in Figure 13.

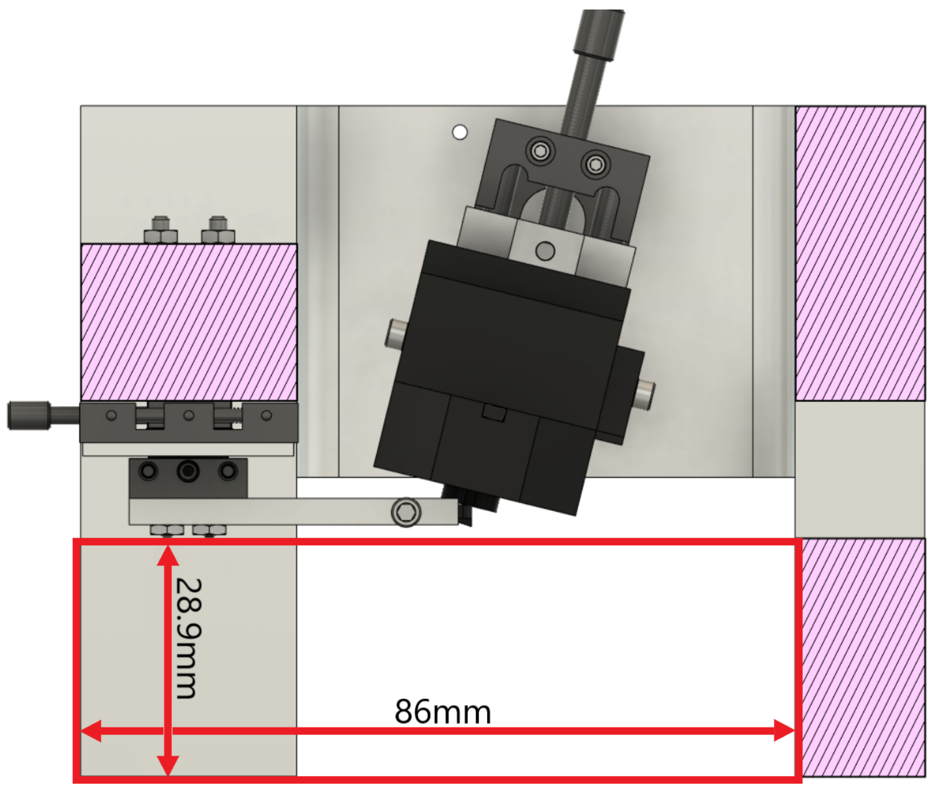

Figure 13: Component alignment and proximity

To test the system as a whole, assembly of the system as it was designed and configured occurred and when challenges presented themselves, adjustments were noted and changes were made to compensate for undesirable behavior. The result is seen in Figure 12.

3.2 Testing Methodology

Testing what was fabricated involved examining what was planned in contrast to what actually came to be. The testing portion of the methodology involved putting each component through its paces and analyzing performance. Prior to assembly and testing of the system as a whole, the individual components needed to be tested. Of particular concern was the ability of the circuit to function since it is far more delicate and complex than the test stand components.

Table 2. Table of experiments for testing noise floor and resolution of the new circuit and OPU based AFM and test stand

Trial	Piezo stimulation voltage	Corresponding change in height
1	5V	12500nm
2	2.5V	625nm
3	1V	250nm
4	500mV	125nm
5	200mV	50nm
6	100mV	25nm
7	50mV	12.5nm
8	0.0V	0nm

To demonstrate the circuit’s ability to function, a test for noise and accuracy of the circuit was performed to illustrate capability of the circuit and examine the noise present in the circuit. Examination of the constructed circuit was done by obtaining FFT data for the system's response to a regular oscillating signal over a set time. The comparison for response is generated by positioning the OPU at the focal point above a surface. The surface oscillated at 1.5Hz in a square using a piezo actuator which was powered by a function generator. Signal data was captured over the course of two minutes through a NI 6002 DAQ device connected to the coax output connection on the circuit, and was written to an Excel file at 70Hz. The table of experiments is seen in Table 2. Each trial reduced the stimulation of the piezo so that the resolution can be determined and quantification of the noise floor achievable. The piezo's response to voltage stimulation was 250nm per 1V.

The setup for testing all circuitry involved using two voltage supplies with each set to output nine volts with the positive output of one of the power supplies connected to the negative of the other. This connection is considered ground. Collectively an 18V difference is achieved. This is the same configuration that was used with the previous breadboard circuit. To tune the circuit into its operation window for amplification of the signal, the output of the circuit which is labeled "CoaxOutput", and corresponds to amplified Equation 2, was connected to an oscilloscope. When the repeating oscillations from the piezo located under the OPU were properly represented on the oscilloscope, it was known that the focal point of the OPU was in the right place for testing. For all operations with the OPU and circuit, this same dual voltage supply setup and oscilloscope combination was used.

Furthermore, a longevity test was used to observe the changes over time and evaluate the consistency of the circuit's power delivery. In this test the OPU was tuned close to its focal point, but at one extreme of the CoaxOutput's amplification capabilities inherent to the circuit's design. The power delivered to one quadrant was monitored over the course of an hour using a multimeter to measure the quadrant's output voltage relative to ground. This test was used to indicate the degree to which the circuit and OPU behave consistently through prolonged use in comparison with the observed decline in total voltage of the bread board as seen in the initial testing of the previous breadboard circuit.

To test the test stand system, its ability to be assembled was the primary concern. Of great importance was ensuring that the pieces fit appropriately, that the unit was as robust as anticipated, as well as tolerant to noise and general movement and assembly stresses. Additionally, should any component become defective or break during assembly it would need to be reassessed, reconfigured, and manufactured again to compensate for its defectiveness.

Chapter 4: Results and Discussion

The Results and Discussion section is separated again into Design and Fabrication, and Testing. First, the results for the design aspect of the thesis are discussed with respect to quality, accessibility and usability, and then the results for functionality, reliability, and accuracy are discussed in the Testing Results section. These sections are followed by a discussion that highlights the capabilities of the instrument and provides insight into the implications the results have with respect to advancing the project.

4.1 Design and Fabrication

In the following sections the Design and Fabrication results are presented. The circuit and test stand with its components were assembled and assessed for basic functionality and usability aspects which are critical for ease of use and access for future modifications as well as tuning. These sections discuss the PCB layout areas for improvement and assess the capacity to perform its primary functions. Furthermore, these sections also discuss the test stand's ease of assembly and modifications necessary to facilitate assembly. Additional design and fabrication results are interspersed as they relate to the methodology and intentions of this project's attempt to further develop a prototype AFM.

4.1.1 Circuit Board Fabrication and Assembly Results

The prototype PCB resulted in improvements in usability and reliability. Through this implementation, areas for further simplification and improvements to the circuit design were identified. Recommendations for future improvements are discussed in the Future Works section of this document. The most notable areas for improving the circuits were with regard to accessibility of the test pins and orientation of the large capacitors due to their large footprint impeding the ability to access the connectors. Figure 14 is a comparison between the bread board implementation and the new circuit developed.

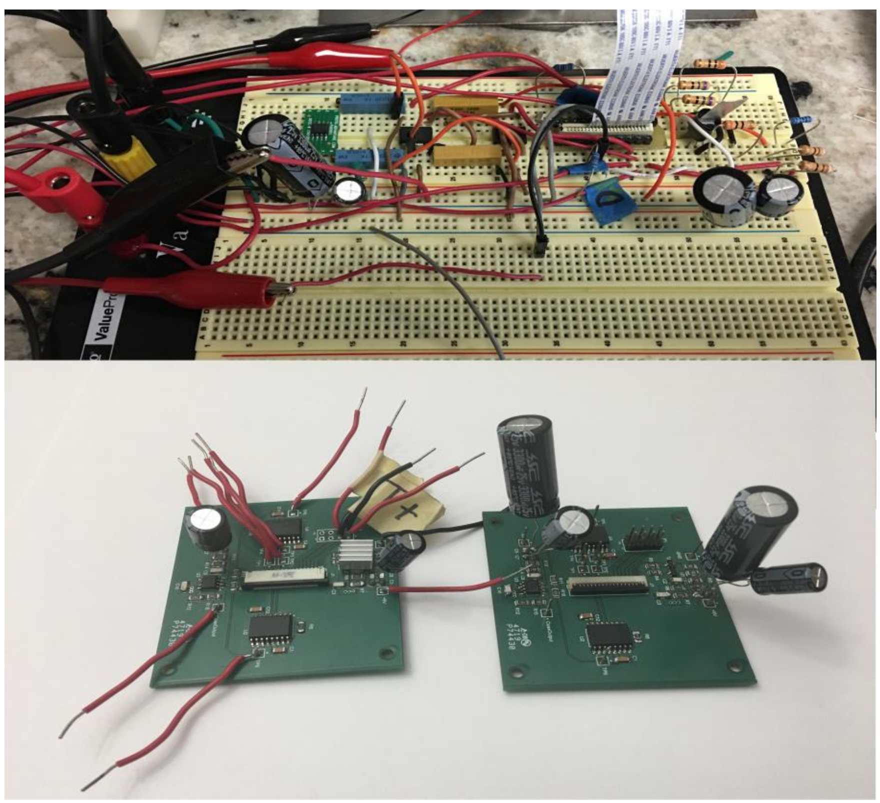

Figure 14: Top: Original breadboard circuit. Bottom: Current circuit boards with circuit 2 on the left and circuit 1 on the right.

4.1.2 From Breadboard to Circuit Board

Changing from a breadboard to a circuit board resulted in minimal changes to the layout. The most impactful differences were in component selection and circuit refinement. In the circuit board configuration, the potentiometers were replaced with resistors, and capacitors were added to the INA217 amplifiers as specified by the manufacturer.

In advancing to this next level of circuit integration, the main benefits are in reliability and robustness and improved plug and play usability. With the correct equipment available, less than 10 minutes are needed to go from completely disconnected to fully integrated and operational, compared to an hour or more of time spent with the previous circuit sorting and tweaking connections until a consistent signal was achieved. Due to the reliability of the fabricated device almost all troubleshooting was eliminated and was exclusive to tweaking only the interface points and ensuring none of the attached wires were contacting one another.

4.1.3 Test Stand

The components fabricated as seen in Figure 15 were machined to specification and fit mostly as intended upon assembly. Each piece was made of aluminum. It was important that these components fit properly so minor modifications needed to be made during fabrication that didn’t interfere with operation or interface between sensitive components. The OPU holder needed an indent at the location of the OPUs diode array to allow for the OPUs inconsistent assembly. Creating a slot approximately 2mm in depth across the portion of the OPU holder contacting the sensors prevented the interference and allowed for the OPU units to be properly mounted as originally intended.

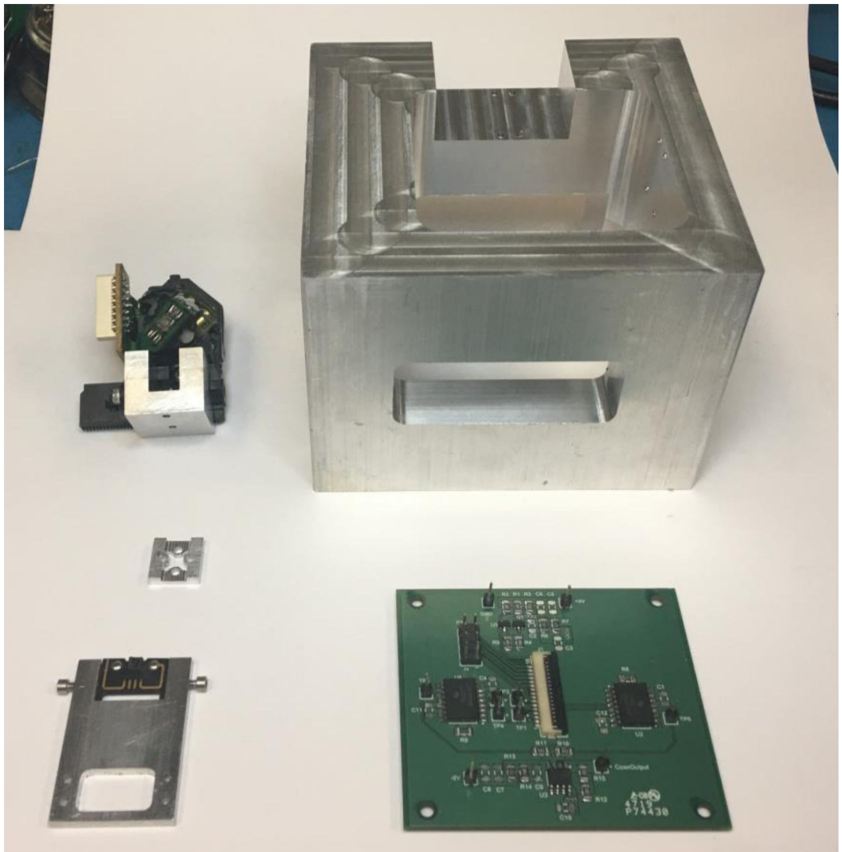

Figure 15: The fabricated and assembled components of the AFM prototype

Assembling the test stand was challenging in the ways that were expected. Due to the small size and close proximity of the components, mounting hardware and tightening the fasteners was difficult and took time and patience. Furthermore, the ability to insert the ribbon cable to the OPU after assembling the test stand was difficult at a minimum. While it was possible to assemble, increased accessibility would likely be preferred in future iterations. Modifying the structure to be more open, and removing one of the non-essential walls would greatly increase accessibility of the components and assemblability. An image of the assembled test stand can be seen in Figure 16.

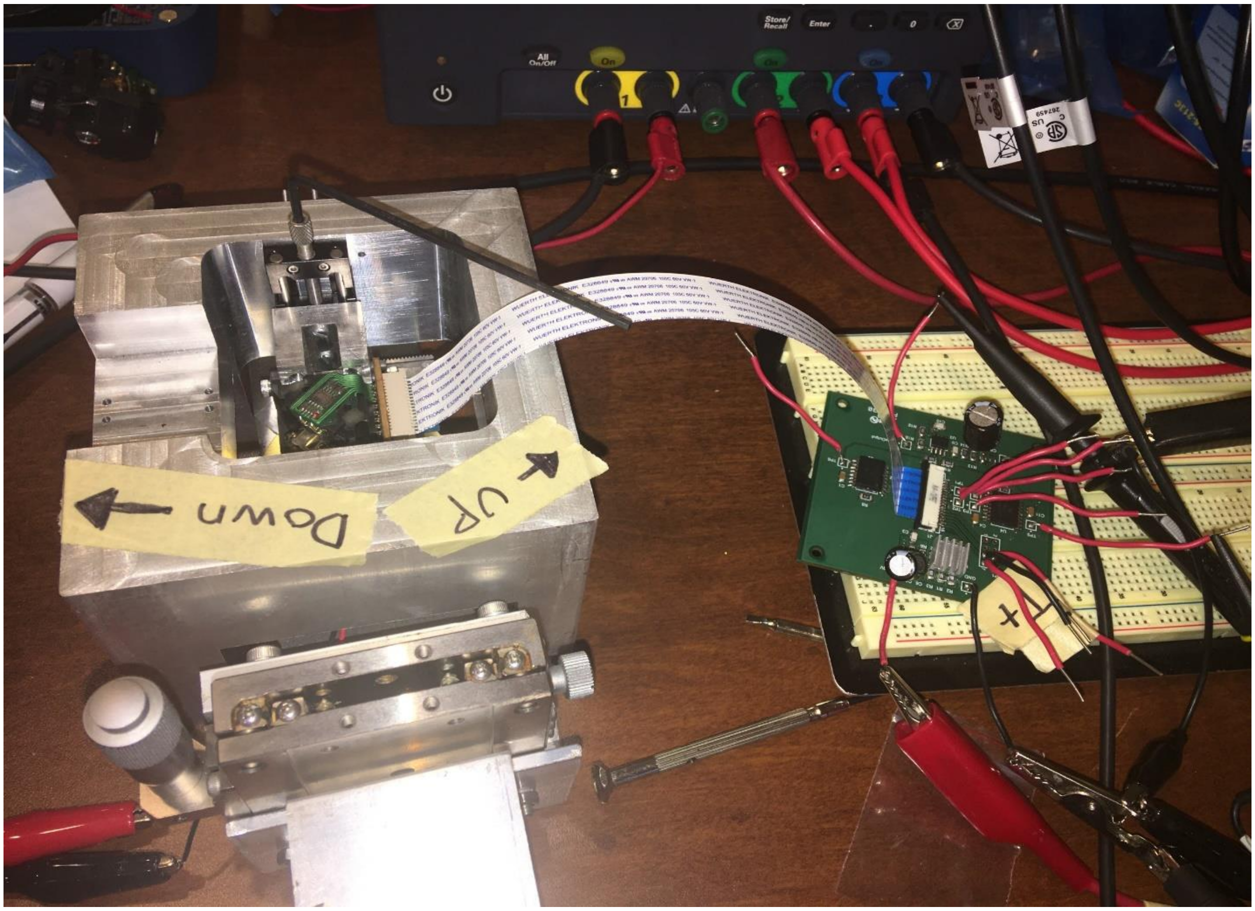

Figure 16: Assembled test stand with circuit

4.1.4 Modifications from Design to Operation

From what was planned to what came to be, the second circuit was assembled with the mistakes of the first in mind, but using the leftover components. The main changes involved substituting soldered pins for wires so they could be more easily gripped with alligator clips.

4.2 Testing Results

The testing results mirror the experiments discussed in the testing methodology section and outline the performance and reliability of the system in comparison with expectations and the performance of the previous system. These experiments looked at the functionality, longevity and accuracy of the circuit that was fabricated. Alignment testing results for the test stand is also discussed at the conclusion of this section.

4.2.1 Functionality of the Circuit

In the testing of the circuit's long-term consistency, the circuit maintained capacity to power the circuit for extended periods of time with minimal deviation in quadrant voltage. This testing lasted an hour and demonstrated consistency in contrast to that exhibited by the breadboard variant shown in Figure 7. The new circuits results are seen in Figure 17.

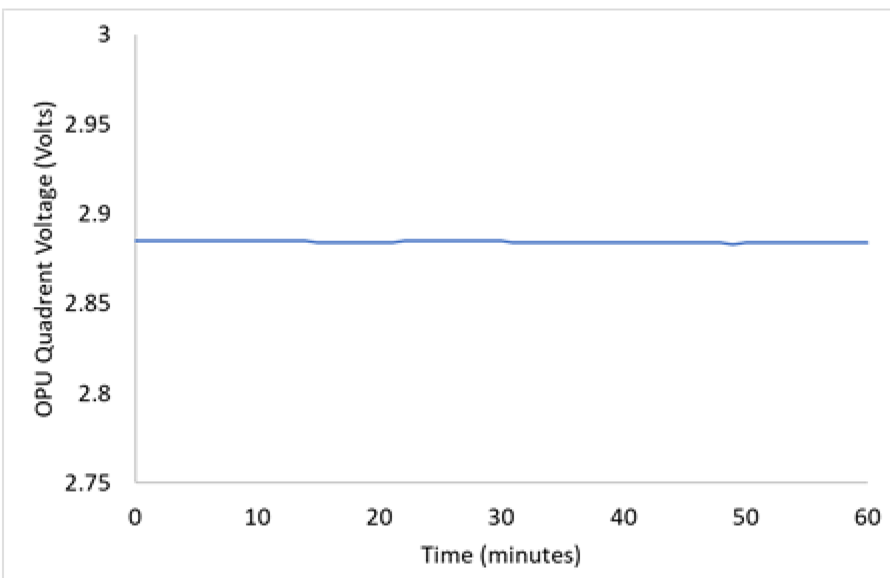

Figure 17: New circuit longevity test results

The difference in the consistency is seen to be several orders of magnitude greater when using a calculated variance for each data set to compare the two. The data for Figure 17 for the new circuit had a calculated sample variance of 2.68E-7, which is much more uniform when compared to the breadboard circuit which exhibited a sample variance of 0.136.

In testing of the amplification of the circuit it was revealed the output was close to what was expected. A function generator producing an oscillating sine wave with a 1mV amplitude was connected to the inputs of the amplifiers on the circuit and produced a peak-to-trough voltage at the CoaxOuput of the circuit of approximately 8.3V, which is within the margin of error. The results align closely with the expected amplification as calculated by Justin Rudie of 4,131 which in this situation would have produced 8.262V from the 1mV input. This 0.46% difference between 8.3V and 8.262V indicates functionality of the circuit's ability to handle the small signal and amplify its results. A snapshot of this amplification is seen in Figure 18.

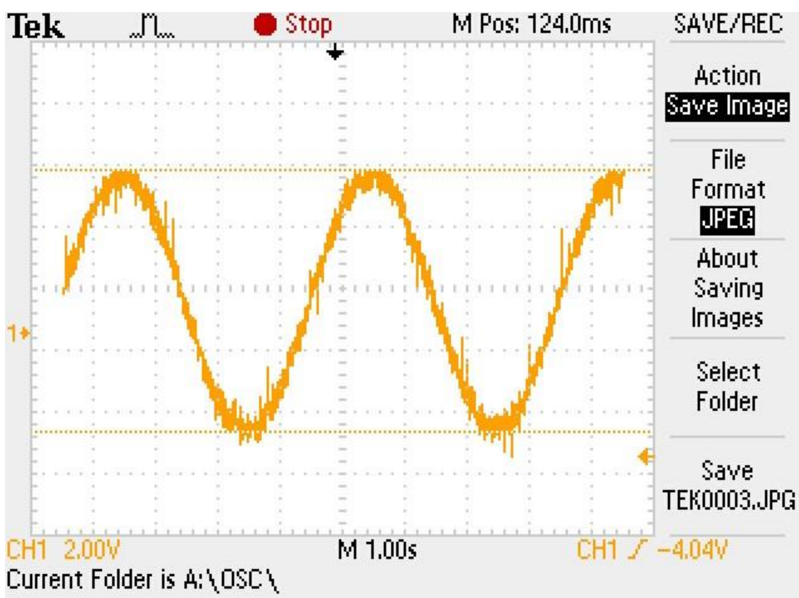

Figure 18: Output of the circuit shown on the oscilloscope. This 8.3V P2P sine wave is the circuit's output for the input of a 2mv P2P sine wave.

4.2.2 Physical Circuit and OPU Test Results

In testing of the system, noise data was collected to examine the true ability of the system to function with a high degree of accuracy. In this test after around 200mV, which corresponds to 50nm of piezo excitation, the signal is seen falling into the noise floor.

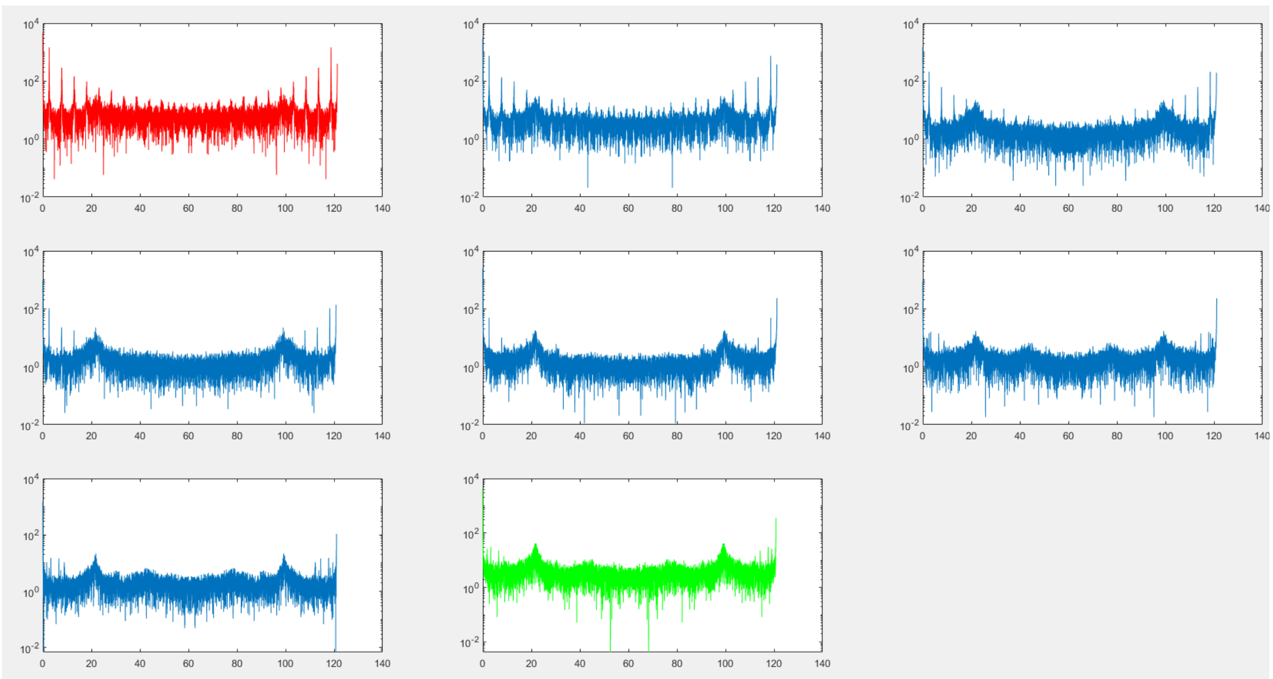

Figure 19: Graphs are arranged in descending order from highest piezo excitation voltage to lowest, from left to right, top to bottom. The excitation voltages are 5V, 2.5V, 1V, 0.5V, 200mV, 100mv, 50mV, 0V. The frequency is 1.5Hz. The X axis is frequency in Hz and the Y axis is dB

As seen in the data in Figure 19, the configuration that was tested, the noise floor is seen overcoming the signal being generated by the piezo and being picked up by the OPU. It is seen that beyond 50nm of travel the signal is no longer distinguishable from the noise floor. This can be more clearly visualized with Figure 20 through a Signal to Noise Ratio (SNR) graph which examines the presence of the signal within each test for each piezo voltage. It is seen that the signal integrity drops from around 20dB to between 5 and 10dB above the noise floor between trials 5 to 6. The 5 to 10dB range is considered to be approximately the minimum range for discerning data in a signal [27]. The data in Figure 20 was created by obtaining the power spectral density of each trial run to obtain the signal power in dB and then noise power in dB and using the formula SNR=(S – N) to calculate the SNR for the 1.5Hz signal in each trial.

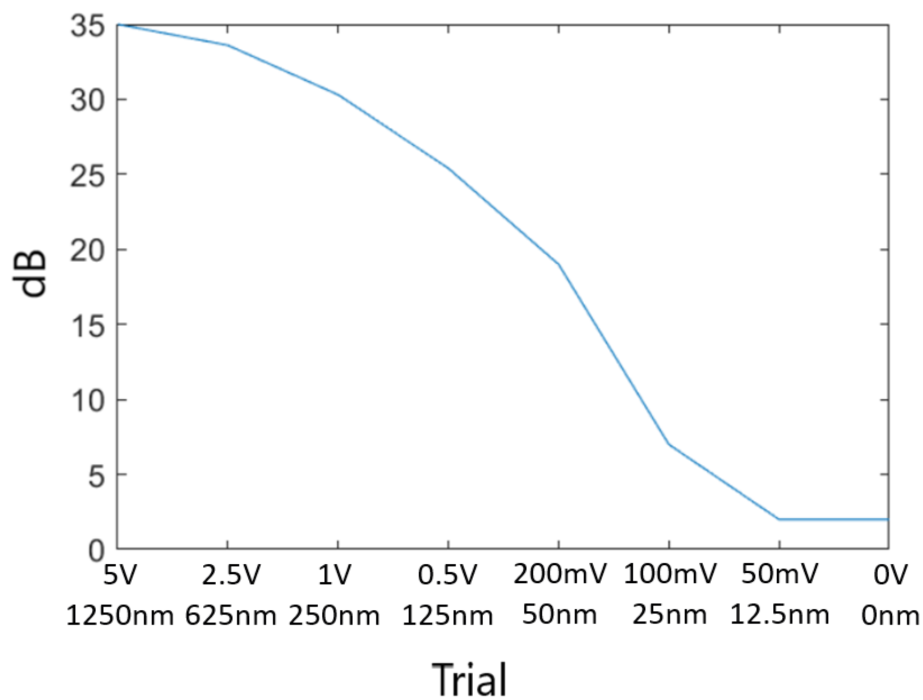

Figure 20: Vertical axis is the net SNR of the Signal with respect to noise floor. The horizontal axis is the trial number corresponding to 5V, 2.5V, 1V, 0.5V, 200mV, 100mv, 50mV, 0V of stimulation for the Piezo actuator.

Additional testing did demonstrate intermittent ability to distinguish the signal for 50mV corresponding to 12.5nm of travel as seen in Figure 21, however this result required careful tuning and was only visible for brief moments at a time.

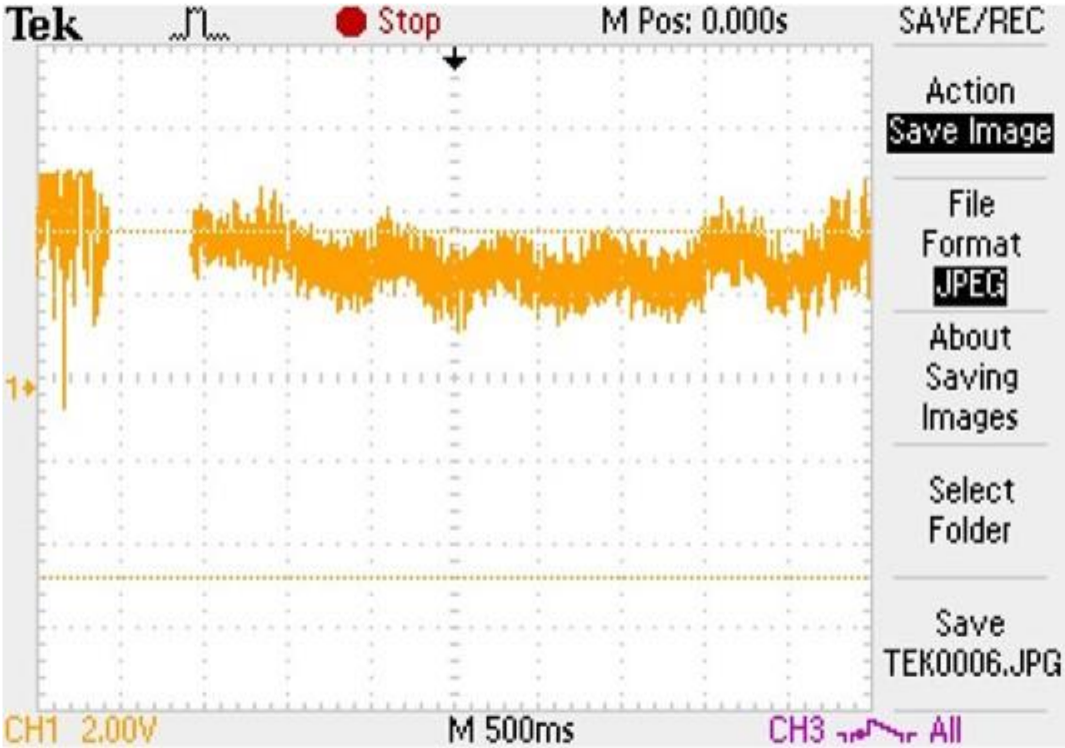

Figure 21: 12.5nm of resolution observed momentarily. This is the circuit's response to a 50mV 1.5Hz sine wave

4.2.3 Alignment of Components of the Test Stand

In testing of the integrated system, it was found that the ability to adjust each piece of the system occurred as expected. While one of the axis for the probe holder was difficult to move it was still possible to make adjustments. Movement of the OPU was also challenging in that the use of a long lever in the form of a hex key Allen wrench was necessary to be able to produce small increments of change detailed enough to tune the focal point so that it was at the right location.

4.3 Discussion

This development endeavor resulted in promising prototype low-cost AFM components, which to the extent of the testing conducted, functioned as intended. The system matches or exceeds the performance of the prior prototype in the areas of robustness, functionality, reliability and accuracy. There is uncertainty with regards to the new system's actual feature resolution capabilities which requires additional testing beyond the scope of this work. The system was found capable of observing disturbances of 25nm reliably, and was capable of intermittently observing disturbances of 12.5nm. Due to the testing having been performed with no noise isolation beyond that which was inherent to the circuit and the test stands, it is conceivable that implementing some traditional methods of noise isolation such as what was used in the previous work in this project would likely result in further improvements in resolution. In all, the system is promising as an affordable AFM solution though it still has plenty of work remaining prior to becoming operational.

Chapter 5: Future Work

The following is the detailed list for what was identified as the most promising and impactful avenues for advancing this endeavor to create a low cost and high-speed atomic force microscope.

A process could be used to reveal the efficacy of the constructed AFM system and help indicate what changes need to be made if any to further iterate on this AFM design. This process would consist of assembly of the test stand, and circuit and probe on the test stand and an attempt to focus the beam of the OPU onto the probe cantilever and then attempt to raise a surface up to the probe tip and observe the cantilever behavior.

Limited access to testing apparatus restricted the ability to use some traditional noise isolation techniques. It would be beneficial to reevaluate the circuit and the test stand's susceptibility to noise under improved isolation such as with insulated granite slabs. All the testing on the new AFM system was performed in a noisy room 15 feet from a furnace, and with no isolation from vibrations apart from the test stand's inherent mass.

Additionally, rebuilding the circuit and better arranging the locations for the test pins would improve accessibility. Furthermore, the CoaxOutput should be an actual coax connection, and moving the ribbon cable connector to the edge of the circuit might also alleviate some of the challenges of inserting the ribbon cable into position. It would also be good to redesign the DC current supply portion of the circuit for the OPU using matched transistors to obtain even more consistent performance. Due to the current draw of these transistors, the transistors had a tendency to heat up. Adding a heatsink marginally mitigated this problem. It would be good to redesign the power delivery with the temperature challenges and power delivery requirements in mind for each component.

One of the challenges with working with the system was accessibility of the components. Removing the side opposite the side in which the OPU is mounted would help with the ability to access the components in the system. Additionally, removing the left leg on that side would allow for reconfiguration of the XY actuator so that the control for the actuator, that is currently facing inwards towards the side that holds the OPU, is accessible. One change that might also help would be changing the angle of the XY probe mover to be perpendicular to the cantilever. Due to the angle in which the probe is mounted to its holder, the probe actuators are actuating on a plane not perpendicular to the plane that the OPU focal point traverses. Changing the angle might alleviate some tuning challenges caused by the current configuration.

There are also several further modifications to the test stand that would improve user experience and functionality. Milling additional material away and incorporating space to more easily replace the ribbon cable would alleviate some frustration with setup. Furthermore, it would likely be worth pursuing the idea of integration of the sample and its piezo actuation system directly into the test stand structure, rather than separating them, as it would further help with the robustness of the system as whole.

It may also be worth investigating the usefulness of the tracking and focus feature of the OPU. Basic testing revealed promising results for precise tuning of the focal point over a surface.

Data acquisition rates are one of the limitations for AFMs, which can be capped by the bandwidth restrictions inherent to their sensors. In the instrument developed here the KSS-213C CD head is intended to be operated at 1.229MHz due to its designed compatibility with CD write and read speeds. In practice, this sampling speed likely outperforms the capabilities of any currently available probes. This means that even at speeds where surface feature variance is well below the Nyquist frequency when scanning, the cantilever wouldn’t be able to properly represent the data and would become the bottleneck.

Due to the cantilever's height positioner behavior and the natural tendencies of the probes, even small cantilevers with higher natural frequencies above 5mhz aren't capable of providing intelligible results, which results in artifacts in the data. At speeds greater than 1.4mm/s it has been seen that even 5Mhz natural frequency probes begins to deliver results with artifacting as a result of parachuting across the surface [28]. With the KSS-213C CD's 1.229Mhz sampling rate for example, data would be taken every 1.1nm which is much quicker than the response rate for a cantilever and positioner to be able to compensate for and produce accurate results.

Increasing accuracy could be done by attempting additional methods of keeping contact with the surface as was discussed earlier in the background section of this paper. However, 1.1nm is fairly tight spacing between sampling and is considered reasonably accurate for a low-cost and high-speed microscope. Increasing frame rate to approach higher video speeds while maintaining a tight spacing between samples ultimately results in the KSS-213C CD becoming a limitation, assuming the cantilever's contact problems have been solved. As such upgrading the optical pickup unit to a higher data-rate alternative such as a 36Mhz Blu-ray or 11Mhz DVD OPU could solve this problem. However, solving the probe's contact problem at high speeds will need to be addressed first, unless the stretched horizontal resolution is acceptable.

Due to an AFM system's complexity, several factors contribute to the degradation of the surface topography data while scanning. Many of these challenges are quantified and discussed in detail with several solutions for each available in AFM literature. Developing low-cost implementations, starting with the most impactful will further enhance accuracy and allow for improved higher frame rates with lower losses. Based on available information the following should be of primary consideration and should be accounted for when analyzing the data: oscillations and hysteresis in the piezo actuators, thermal noise in the cantilever, probe contact, and elevation controller characteristics. Due to the relatively consistent and quantifiable behavior of these perturbations, they are mostly capable of being modeled and filtered out of the data retroactively. Alternatively, implementing measures to eliminate the challenges proactively would likely achieve similar results. An example of something that would need to be accounted for proactively is tuning the proportional integral controller used to keep the cantilever on the surface. The challenge is to achieve high probe to surface return rates with minimal or no oscillations or overshoot.

Chapter 6: Conclusion

A low-cost prototype housing, distance measurement unit, and PCB amplification circuit were fabricated and tested for use as a low-cost and high-speed AFM instrument. Testing of the prototype components yielded promising results matching or exceeding the results of the preceding prototypes that utilized less robust versions of the components developed in this thesis. When these components were tested as a system, 12.5nm of vertical resolution was clearly visible with increased resolution probable if it were to be deployed in a lower noise environment. The efforts here further demonstrate advancement in, and viability of, low cost and high-speed AFMs. The prototype components produced for this thesis' successful operation sets the stage for the completion of the final steps needed for assembly of a functional but developmental AFM. While methods of observation other than those of the scanning probe variety, such as optical or electron microscopy have filled many gaps in understanding of the microscopic world, limitations inherent to each method leave room for techniques such as high-speed atomic force microscopy to lead the way in further discoveries. The works discussed in this thesis are a basis for creation of such an atomic force microscope instrument that could be made readily available to the general public with the potential to be used in studies that could further deepen the world's knowledge.

References

[1] J. S. Slifies and S. A. Schwartz, "The Diffraction Barrier in Optical Microscopy," *Nikon's MicroscopyU*. [Online]. Available: MicroscopyU, https://www.microscopyu.com/techniques/super-resolution/the-diffraction-barrier-in-optical-microscopy [Accessed Dec. 15, 2020].

[2] T. Richards, H. Richards, A. Richards, and M. Weschler, "Best Scanning Electron Microscope Prices | TSS Microscopy," 2021. [Online]. Available: https://www.tssmicroscopy.com/instruments/categories/scanning-electron-microscopes/. [Accessed Feb. 12, 2021].

[3] O. Krause, "AFM Probe Manufacturing Nanoworld tip technology." NanoWorld Services GmbH.

[4] "CD/VCD PICKUP SPECIFICATIONS MODEL:KSS-213C(FOR KSM-213CCM)." Smartech Electronics and Machinery Manufacturing Co. , Zhuhai.

[5] H.-S. Liao, K.-Y. Huang, I.-S. Hwang, T.-J. Chang, W. W. Hsiao, H.-H. Lin, E.-T. Hwu, and C.-S. Chang, "Operation of astigmatic-detection atomic force microscopy in liquid environments," *Review of Scientific Instruments*, vol. 84, no. 10, p. 103709, 2013.

[6] J. Rudie, "OPU Based AFM Design and Optimization Research," thesis, 2019.

[7] Sample Preparation for Atomic Force Microscopes: Recorded Seminar. 2016.

[8] K. Amporndanai, "Biological Specimens Preparation for X-ray Microscopy," thesis, 2014.

[9] E. E.-T. H. En-Te Hwu and A. boisen, "Hacking CD/DVD/Blu-ray for Biosensing," 2018.

[10] "Capabilities," *ICSPI*. [Online]. Available: https://www.icspicorp.com/capabilities. [Accessed Dec. 8, 2020].

[11] G. Shan, Z. Song, Y. Li, and L. Zhang, "A homemade atomic force microscope based on a quartz tuning fork for undergraduate instruction," 2016.

[12] S. Necipoglu, S. A. Cebeci, E. Has, L. Guvenc, and C. Basdogan, "A Robust Repetitive Controller for Fast AFM Imaging." 2012.

[13] A. Liebig, A. Peronio, D. Meuer, A. J. Weymouth, and F. J. Giessibl, "High-precision atomic force microscopy with atomically-characterized tips," *New Journal of Physics*, vol. 22, no. 6, p. 063040, 2020.

[14] V. Bučinskas, T. Lenkutis, I. Morkvėnaitė-Vilkončienė, and V. Kovalevskyi, "Increasing Imaging Speed and Accuracy in Contact Mode AFM," 2019.

[15] M. S. Rana, H. R. Pota, and I. R. Petersen, "Improvement in the Imaging Performance of Atomic Force Microscopy: A Survey," 2017.

[16] Techniques to Reduce EMI In Your PCB Designs, 26-Mar-2020. [Online]. Available: https://resources.pcb.cadence.com/blog/techniques-to-reduce-emi-in-your-pcb-designs-2. [Accessed Dec. 15, 2020]

[17] H. Alemansour, M. Maroufi, A. Alipour, and S. O. RezaMoheiman, "A Feedback Controlled MEMS Probe Scanner for On-chip AFM," 2019.

[18] A. Dzedzickis, V. Bucinskas, D. Viržonis, N. Sesok, A. Ulcinas, E. Sutinys, S. Petkevicius, J. Gargasas, and I. Morkvenaite-Vilkonciene, "Modification of the AFM Sensor by a Precisely Regulated Air Stream to Increase Imaging Speed and Accuracy in the Contact Mode," 2018.

[19] R. Liang, "Design considerations for system-level ESD circuit protection." Texas Instruments Incorporated, Dallas, 2012.

[20] P. Rako, "3 ways to reduce power supply noise"*Electronic Design*, 2019. [Online]. Available: https://www.electronicdesign.com/power-management/power-supply/article/21808839/3-ways-to-reduce-powersupply-noise. [Accessed Dec. 15, 2020].

[21] T. J. Sobering, "Non-ideal Behavior of Feedback Amplifiers DC Errors and Large-Signal Operation." Kansas State University, Manhattan, 2014.

[22] C. P. Papavassiliou, "Noise," in *Instrumentation*, London: Imperial College, 2008, pp. 2–1-2–16.

[23] C. Cassiolato, "How shielding can help minimize noises," *SMAR*. [Online]. Available: https://www.smar.com/en/technical-article/how-shielding-can-help-minimize-noises. [Accessed Dec. 15, 2020].

[24] S. User, "Getting the highest AFM resolution location, location, location," 23-Oct-2019. [Online]. Available: https://www.afmworkshop.com/site-map/articles/109-technical-notes/330-getting-the-highest-afm-resolution-location-location-location. [Accessed Mar. 25 2021].

[25] "Vibration Isolation Solutions to Eliminate Noise in AFM and SPM," *AZoNano.com*, 2013. [Online]. Available: https://www.azonano.com/article.aspx?ArticleID=3254. [Accessed Dec. 15, 2020].

[26] T. Pham and M. Ganzer , “Design and Validation of a Low Cost High Speed Atomic Force Microscope ,” 2017.

[27] “What is Signal to Noise Ratio and How to calculate it?,” *Cadence*. [Online]. Available: https://resources.pcb.cadence.com/blog/2020-what-is-signal-to-noise-ratio-and-how-to-calculate-it. [Accessed Dec. 15, 2020].

[28] H.-S. Liao, Y.-H. Chen, R.-F. Ding, H.-F. Huang, W.-M. Wang, E.-T. Hwu, K.-Y. Huang, C.-S. Chang, and I.-S. Hwang, “High-speed atomic force microscope based on an astigmatic detection system,” *Review of Scientific Instruments*, vol. 85, no. 10, p. 103710, Oct. 2014.